EVLA Memo No. 56
Mosaic Mode Imaging Simulations with the EVLA E and D Configurations

L. Kogan, F. Owen

National Radio Astronomy Observatory, Socorro, New Mexico, USA *

March 26, 2003

Abstract

We carried out a comparison of the design EVLA compact configuration (EVLA-E) with VLA-D configuration. Observation of a trial model image (CAS-A) has been simulated for both arrays using a mosaic mode. A simulated Green Bank Telescope (GBT) image was used to restore the low UV components. EVLA-E configuration was found to be superior to VLA-D in all considered cases. The classical AIPS package was used for the observation simulation, image restoration, and its fidelity estimation.

1 Array description.

The Expanded Very Large Array (EVLA) project is expected to include the compact configuration (EVLA-E). In this memo we compare the imaging quality of the EVLA-E configuration located near the VLA center (figure 1) and with that of the VLA-D configuration using a mosaic mode. The size of the E-configuration array is approximately 250 meters. Eleven existing antenna pads (red circles in figure 1) are used. The positions of the remaining 16 antennas (blue circles figure 1) are optimized to minimize the side lobes inside the primary beam of the 25 meter dish. The maximum positive side lobe inside of the primary beam is 12% (5%) at an overhead snapshot observation, as opposed to 60% (25%) for VLA-D. The numbers in parentheses correspond to the case when the synthesized beam is multiplied by the primary beam envelope. Figure 3 shows the uv coverage of the EVLA-E configuration for different source declinations.

Figures 2 and 4 show configuration and the uv coverage of another configuration EVLA-E-30 at different source declinations. This configuration is designed for observations of southern sources, such as the Galactic center ($\delta < -20^\circ$). Four additional antenna pads along the north arm of VLA are used in this configuration. This configuration has longer spacing at the N-S direction and as a result has less blockage and a more circular beam at low declinations. Tables 1 and 2 show the loss of sensitivity because of the antenna blockages for the EVLA-E and EVLA-E-30 configurations. It is seen from the tables that the EVLA-E-30 configuration has twice the sensitivity near a declination of -30 degrees. Comparison of the UV coverage of the two configurations (figures 3, 4) shows that EVLA-E-30 configuration has a more circular beam at declination $\sim$ -30 degrees. EVLA-E-30 produces 25 % better fidelity than EVLA-E for a declination of -30 degrees when the CAS-A image is restored (figure 8).

*The National Radio Astronomy Observatory is a facility of the National Science Foundation, operated under cooperative agreement by Associated Universities, Inc.

Table 1: Sensitivity Considering Shadowing for Configuration EVLA-E

	Hour Angle, hours								
Decl., deg	-4.	-3.	-2.	-1.	0.	1.	2.	3.	4.
70.	0.96	1.00	1.00	1.00	1.00	1.00	1.00	1.00	0.89
60.	0.96	1.00	1.00	1.00	1.00	1.00	1.00	1.00	0.96
50.	0.96	1.00	1.00	1.00	1.00	1.00	1.00	1.00	1.00
40.	0.93	1.00	1.00	1.00	1.00	1.00	1.00	1.00	0.96
30.	0.89	1.00	1.00	1.00	1.00	1.00	1.00	1.00	0.89
20.	0.89	1.00	1.00	1.00	1.00	1.00	1.00	1.00	0.85
10.	0.74	0.96	1.00	1.00	1.00	1.00	1.00	0.93	0.81
0.	0.59	0.89	1.00	1.00	1.00	1.00	1.00	0.85	0.56
-10.	0.41	0.70	0.85	0.96	1.00	0.96	0.93	0.70	0.41
-20.	0.30	0.59	0.78	0.70	0.70	0.85	0.81	0.52	0.22
-30.	*****	0.26	0.44	0.59	0.59	0.56	0.44	0.22	*****
-40.	*****	*****	0.26	0.33	0.22	0.30	0.26	*****	*****

Table 2: Sensitivity Considering Shadowing for Configuration EVLA-E-30

	Hour Angle, hours								
Decl., deg	-4.	-3.	-2.	-1.	0.	1.	2.	3.	4.
70.	1.00	1.00	1.00	1.00	1.00	1.00	1.00	1.00	1.00
60.	1.00	1.00	1.00	1.00	1.00	1.00	1.00	1.00	1.00
50.	1.00	1.00	1.00	1.00	1.00	1.00	1.00	1.00	1.00
40.	0.96	1.00	1.00	1.00	1.00	1.00	1.00	1.00	0.96
30.	0.96	1.00	1.00	1.00	1.00	1.00	1.00	1.00	0.93
20.	0.96	1.00	1.00	1.00	1.00	1.00	1.00	1.00	0.93
10.	0.85	0.96	1.00	1.00	1.00	1.00	1.00	0.96	0.93
0.	0.70	0.93	1.00	1.00	1.00	1.00	1.00	0.96	0.78
-10.	0.67	0.85	0.96	1.00	1.00	1.00	1.00	0.85	0.67
-20.	0.48	0.81	0.96	1.00	1.00	0.96	0.93	0.74	0.44
-30.	*****	0.56	0.81	0.96	1.00	0.85	0.78	0.44	*****
-40.	*****	*****	0.56	0.56	0.48	0.70	0.52	*****	*****

2 Simulation, image deconvolution and fidelity estimation.

The AIPS task VTESS has been used to carry out deconvolution of mosaic observations using the maximum entropy method. The task was enhanced by increasing the maximum number of pointings from 55 up to 4096. The CAS-A model image of 512x512 pixels is shown in figure 5. The simulation of mosaic observations was carried out for each array using the AIPS simulation task UVCON. Simulated GBT observations were used to restore the short-spacing hole for all simulations. The wavelength $\lambda = 20$ cm. At this wavelength the width of of the 25 meter antenna beam pattern is $\simeq 30$ arcmin. Thus we chose 15 arcmin as the pointing step for the mosaic. Two mosaic sizes were simulated: 7x7 (for which the model size is ~ 1.5 degrees) and 15x15 (for which the model size is ~ 3 degrees). The model cell size was 20" for the 7x7 mosaic and 40" for the 15x15 mosaic. Such cell sizes provide good source coverage. The CAS-A image was convolved with a beam of 153"x153" corresponding to the array angular resolution.

The 15x15 mosaic (cellsize of the model is 40") was used to get better angular resolution compared to 7x7 mosaic because fewer pixels are smoothed out in the convolution with the same array beam 153"x153". While better angular resolution could be achieved by increasing the antenna and array sizes, we prefered to adhere to actual VLA-D and EVLA-E specifications. The VTESS output image was convolved with the same size beam 153"x153". So 4x4 and 8x8 pixels were smoothed out at 15x15 and 7x7 mosaic respectively. Figures 6 and 7 show the convolved model images for cellsize 20" and 40".
The fidelity (FIDELITY) of the restored image is defined as the ratio of the convolved model image maximum to the r.m.s of the difference of the convolved restored image and convolved model image. The parameter FIDELITY was used to estimate array quality. Greater FIDELITY corresponds to better imaging quality. Two types of simulated mosaic observations were carried out: snapshot mosaic when each pointing was observed only once, and multicycle mosaic when several (9) snapshot mosaic observation cycles were made. In the multicycle mosaic all observations with the same pointing were combined together by the task DBCON. The task IMAGR creates 7x7=49 or 15x15=225 dirty maps and beams as input images for the deconvolution task VTESS. The simulated GBT image of the input model and its beam were used as 50th or 226th input image/beam for VTESS.
The whole process of simulation includes:

Simulate mosaic observations (task UVCON)
Combine the same pointing observations to the same UV data (task DBCON)
Prepare 7x7+1 or 15x15+1 images/beams for VTESS (task IMAGR)
For VLA-D the uv tapering is used in IMAGR to get the same array resolution (153"x153")
Convolve output of VTESS with the array resolution beam (153"x153") (task CONVL)
Subtract the restored convolved image from the CAS-A convolved model (task COMB)
Estimate r.m.s. of the difference map (task IMEAN)

Repeat all the above steps for each declination. All the above steps are coded in the AIPS procedure.

3 Results

Figure 8 shows the restored image fidelities at declinations ranging from $-30°$ to $70°$ for the 7x7 snapshot mosaic. All three configurations are plotted. The figure demonstrates the obvious advantage of the compact configuration EVLA-E over the VLA-D configuration. The EVLA-E-30 configuration suggested for the Galactic center observation shows advantage at the -30 degrees declination.

Figure 9 shows the the restored image fidelities at declinations ranging from $-30°$ to $70°$ for 9 cycle 7x7 mosaic. Here again we see an advantage of the compact configuration EVLA-E over the VLA-D configuration. This advantage is not as prominent as in the case of the snapshot mosaic. The observations at each pointing were spread over 6 hours. Thus UV coverage of EVLA-E is still better than VLA-D though not as significantly as for snapshot observations.

Figure 10 shows the restored image fidelities at declinations ranging from -30 to 70 degrees for 15x15 snapshot mosaic. Here again we see an advantage of the compact configuration EVLA-E over the VLA-D configuration. This advantage is not as prominent as for the 7x7 mosaic.

Figure 11 illustrates the restored image quality for compact configuration EVLA-E. The left column shows 7x7 mosaic simulation corresponding to the model cellsize 20". The right column shows 15x15 mosaic simulation corresponding to the model cellsize 40". The upper row shows the restored images, while the lower row shows the relevant models. **The restored images and the relevant models are practically identical on this scale.**

Figure 12 demonstrates the differences between the restored images and the models for the two columns on the figure 11. Again the left column shows 7x7 mosaic simulation. The right column shows 15x15 mosaic simulation. The upper row shows the differences for the compact array EVLA-E. The lower row demonstrates the differences for the VLA-D array. **The advantage of the designed compact array EVLA-E over VLA-D array is obvious.** All simulations were carried out with no thermal noise added. Adding noise for the 7x7x1 mosaic shows no change to the fidelity ratio providing the noise is not greater than the source brightness.

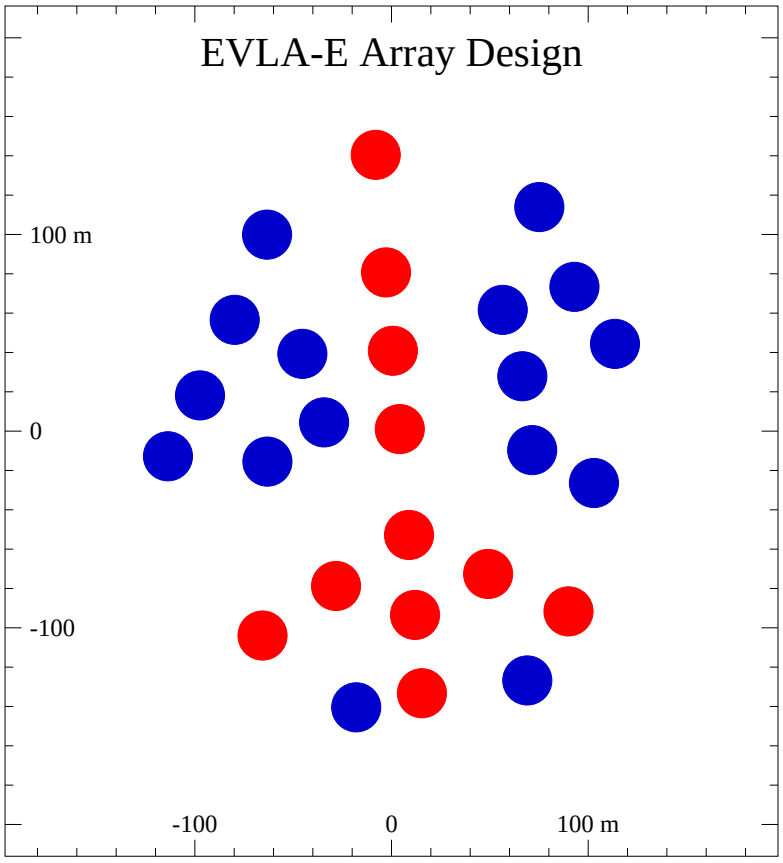

Figure 1: The designed compact configuration EVLA-E. The red circles are the existing VLA pads. The blue circles are the new antenna pads. The circle diameters on the plot correspond to the antenna diameter 25m. The configuration is slightly expanded to north to increase the range of source declinations. The side lobes are optimized inside of the primary beam (maximum side lobes $\sim$ 5%)

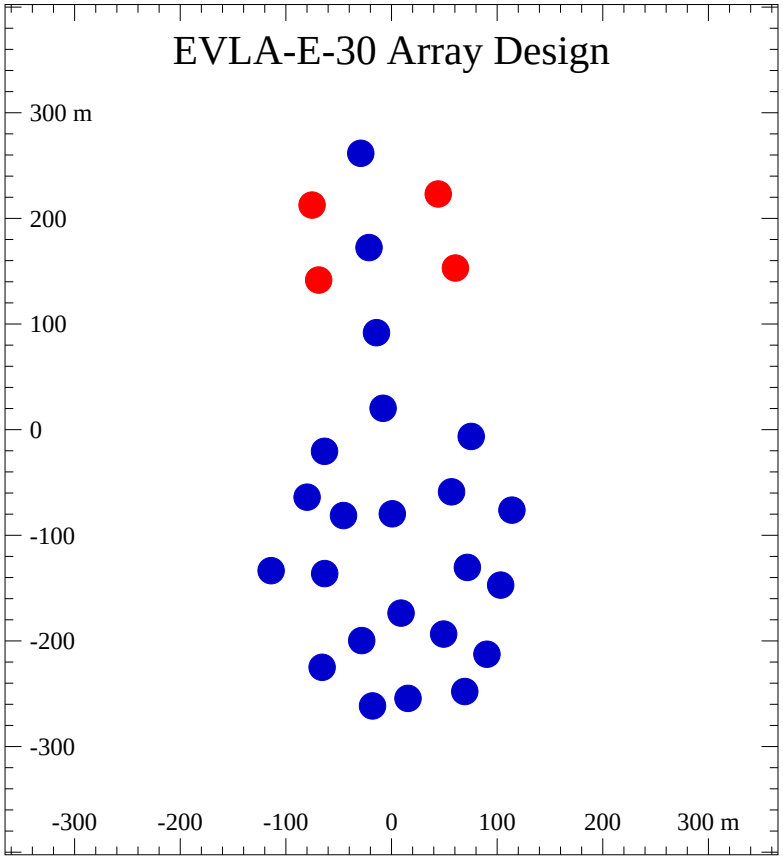

Figure 2: The compact configuration EVLA-E-30 designed for observation of the Galactic center ($\delta \sim -30°$). The blue circles are the VLA pads and pads belonged to the configuration EVLA-E . The four red circles are the new antenna pads. The circle diameters on the plot correspond to the antenna diameter 25m.

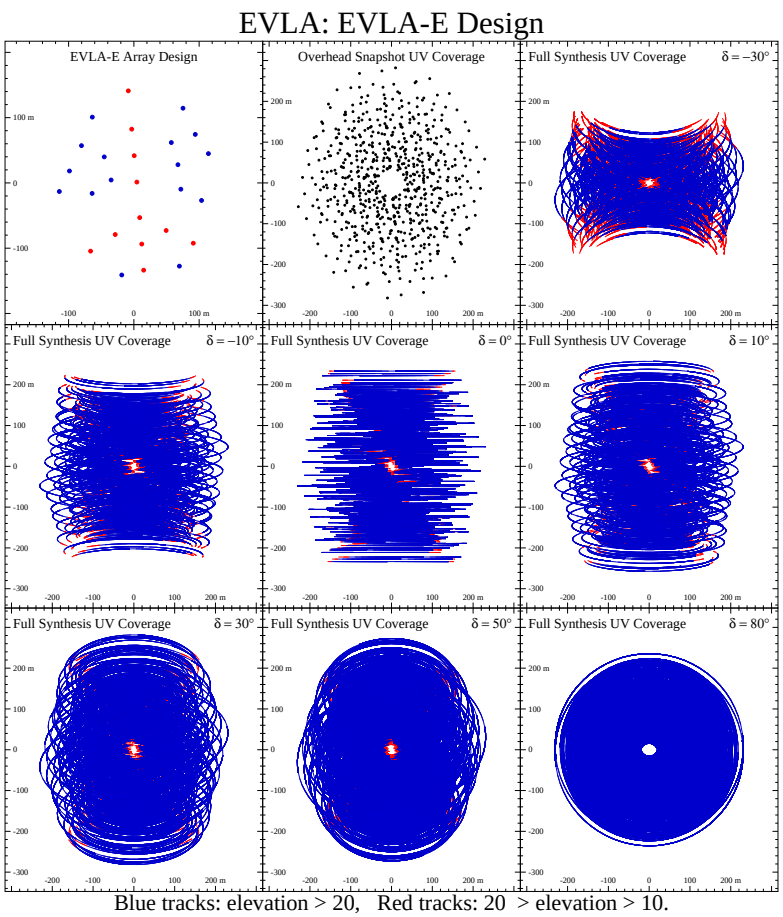

Figure 3: The UV coverage of the designed compact configuration EVLA-E for different source declinations.

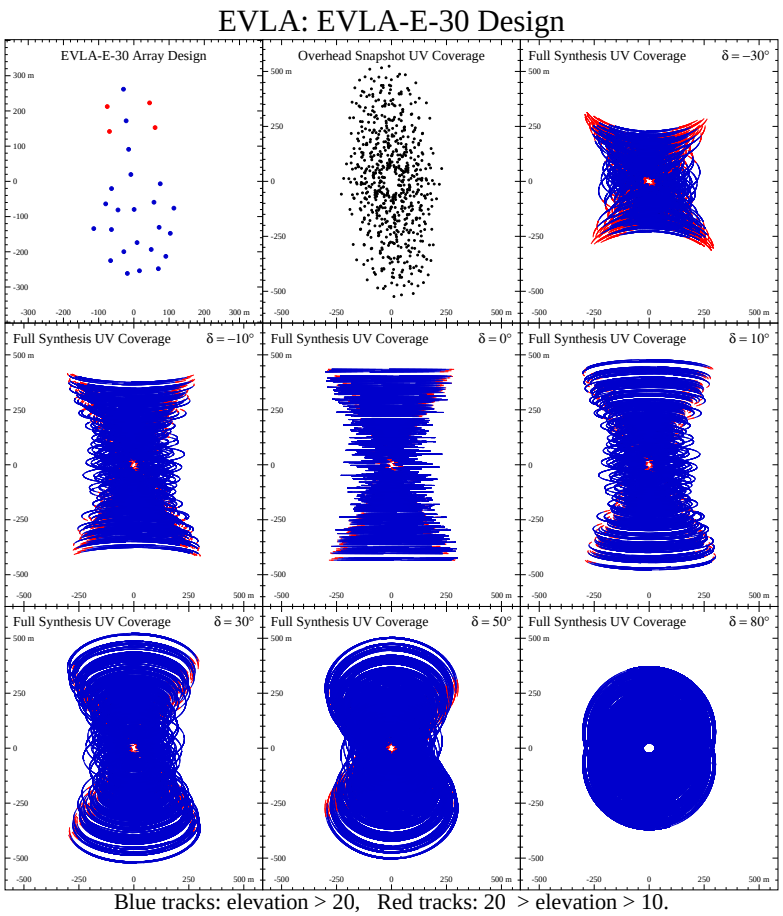

Figure 4: The UV coverage of the compact configuration designed for the Galactic center ovservation.

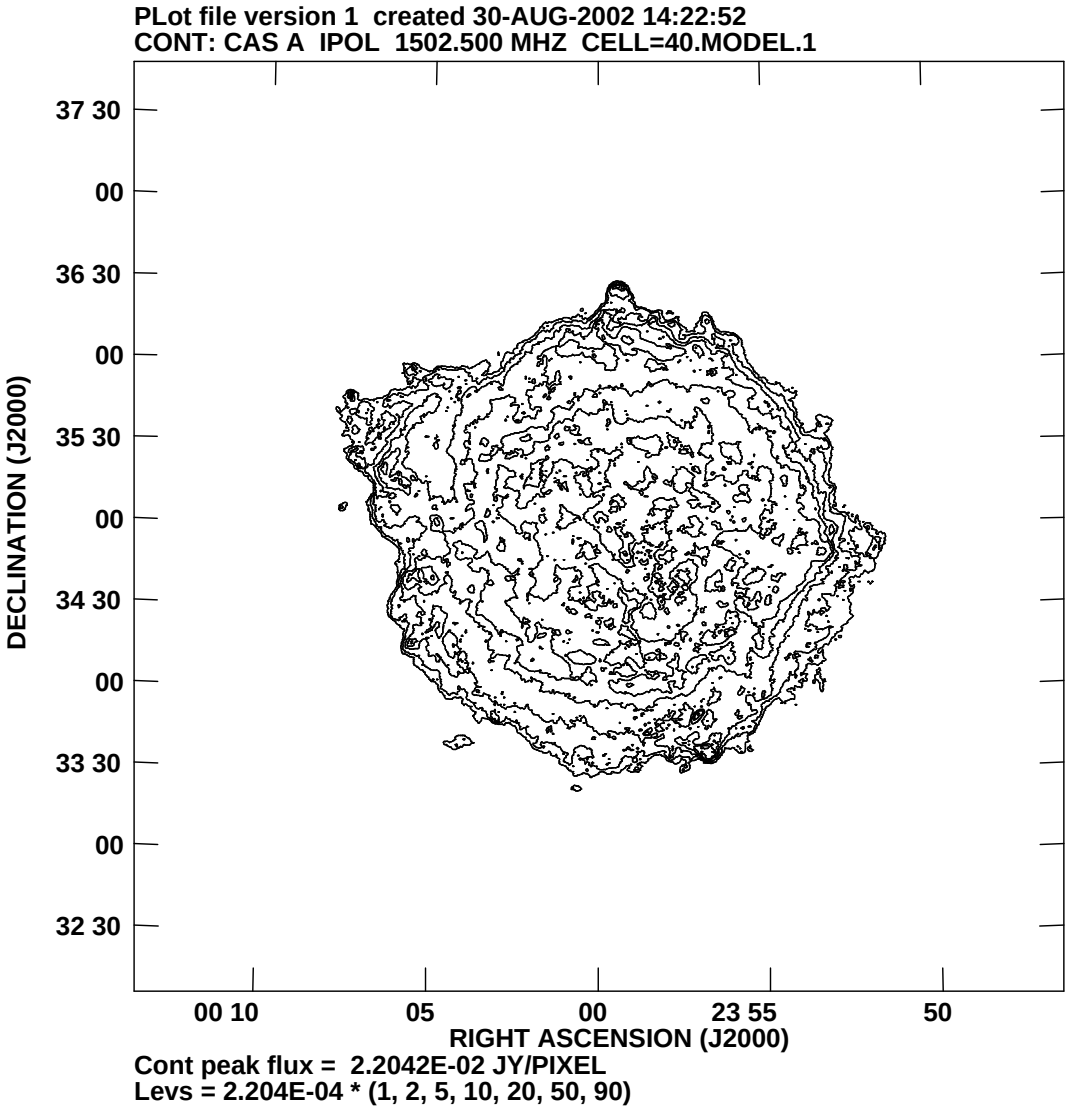

Figure 5: The CAS-A image used as initial model for simulation. Size of the cells was changed from 20" to 40" to have the different number of pixels smoothed at the convolution with the array beam (153"x153"). The cellsize 20" was used for mosaic 7x7 and produced 8x8 pixels smoothing at the convolution. The cellsize 40" was used for mosaic 15x15 and produced 4x4 pixels smoothing at the convolution giving the better discrimination of the fine structure of the model.

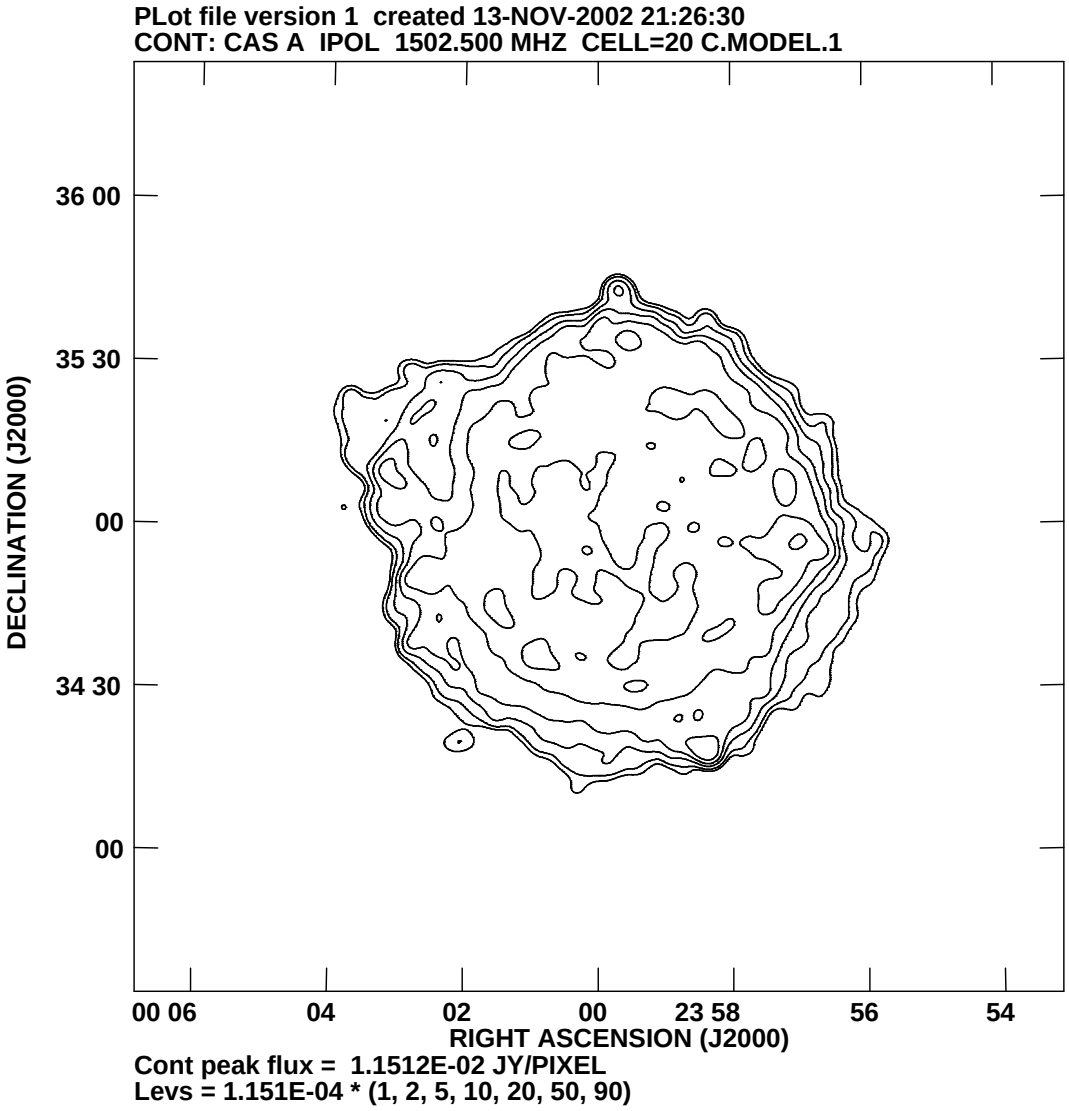

Figure 6: The image of initial model (cellsize=20") convolved with the array beam (153"x153"). Approximately 8x8 pixels are smoothed.

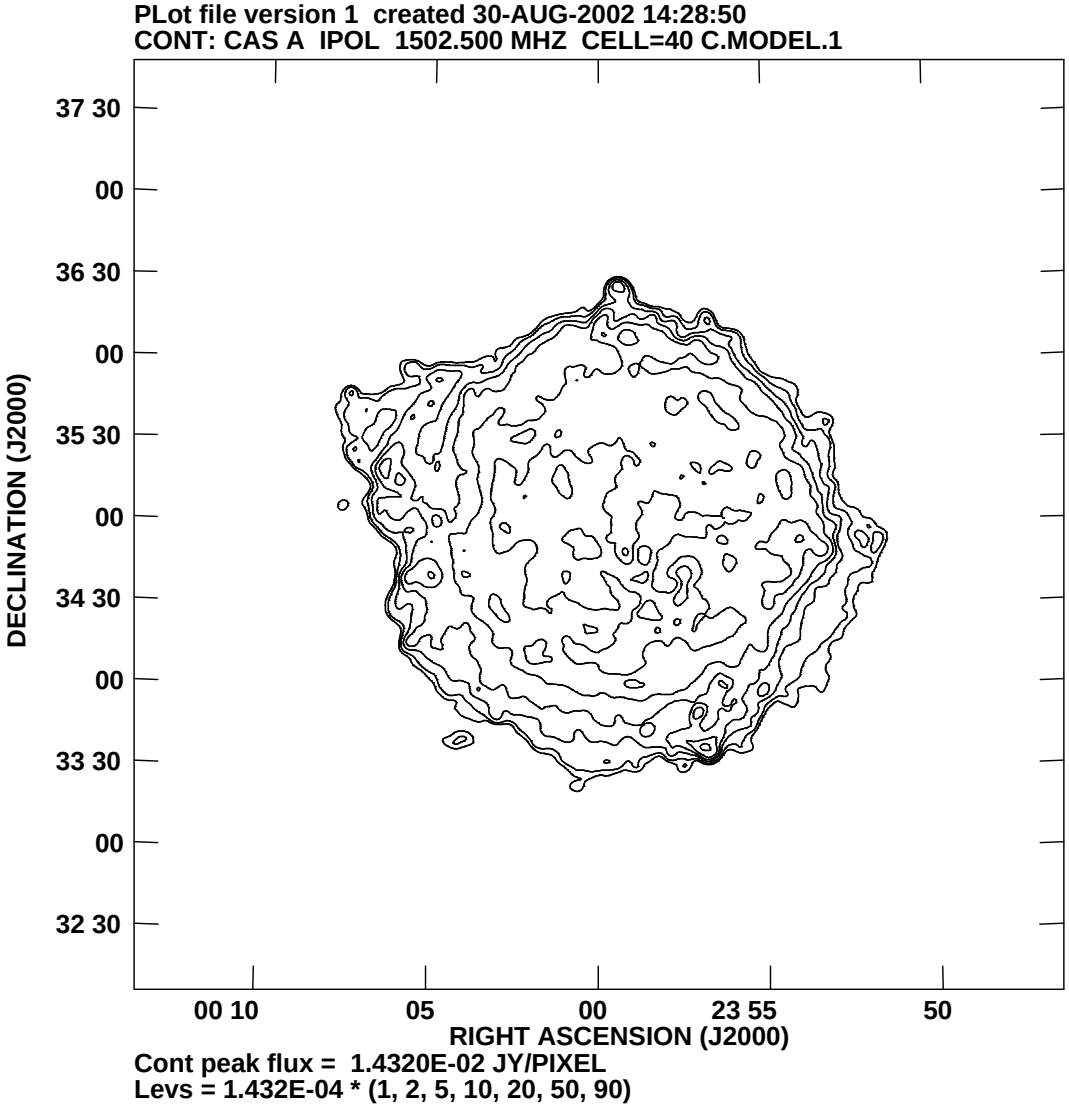

Figure 7: The image of initial model (cellsize=40") convolved with the array beam (153"x153"). Approximately 4x4 pixels are smoothed.

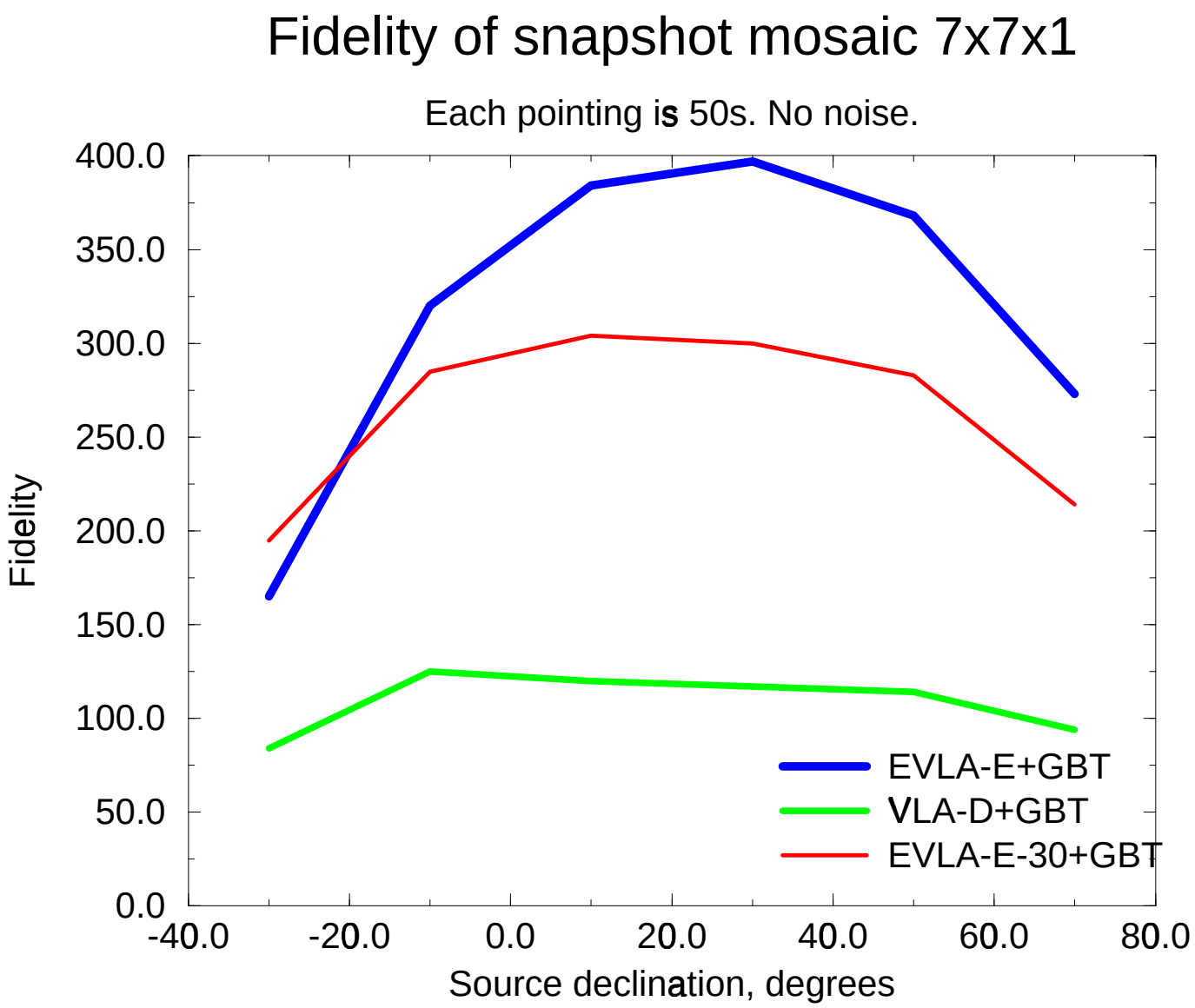

Figure 8: The fidelity versus the source declination for the three considered configurations for 7x7 snapshot mosaic. The advantage of the design compact configuration EVLA-E over the VLA-D is obvious. The configuration suggested for the Galactic center observation (EVLA-E-30) shows advantage at the declination -30degrees.

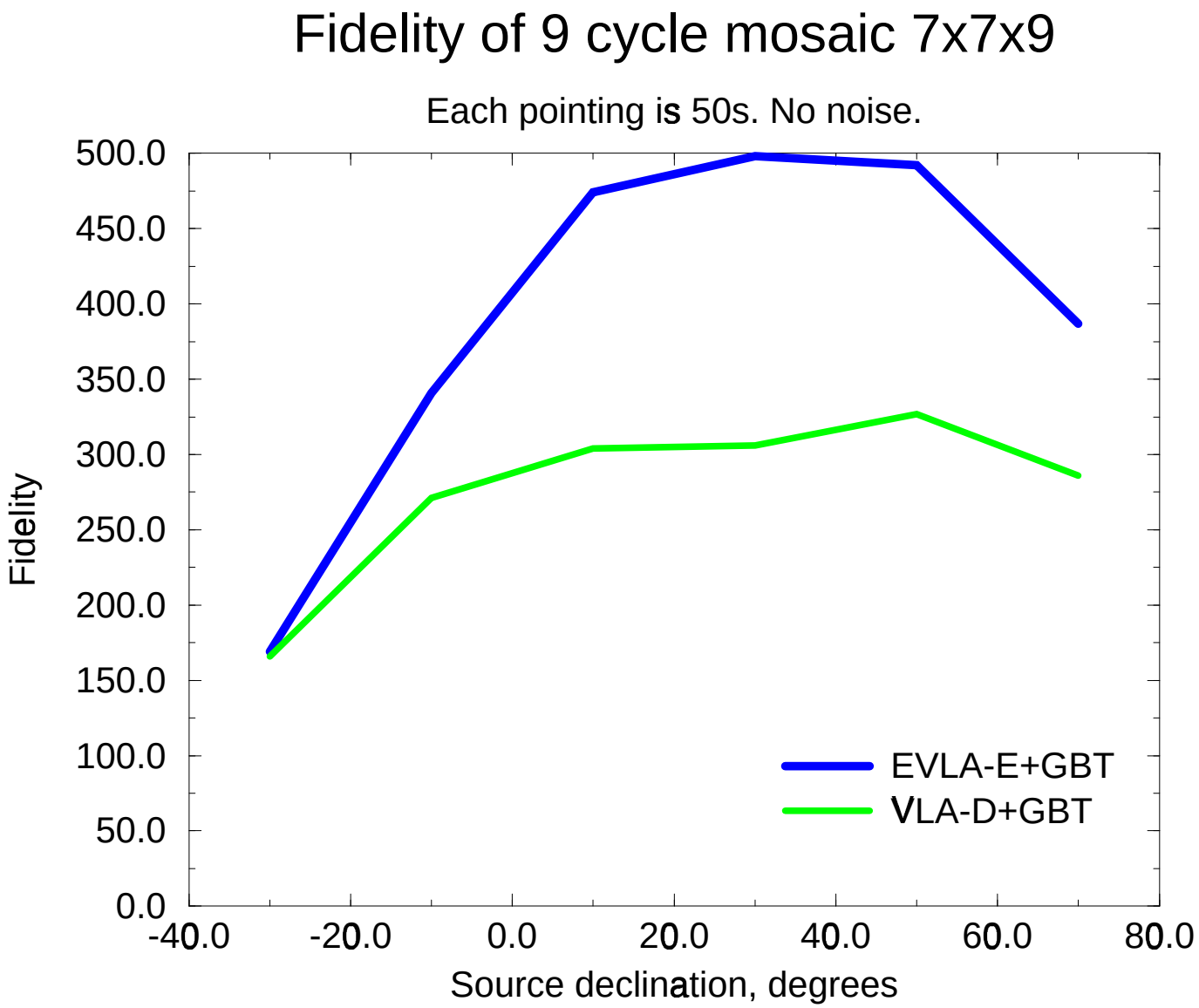

Figure 9: The fidelity versus the source declination for EVLA-E and VLA-D configurations for 9 cycle 7x7 mosaic. The advantage of the design compact configuration EVLA-E over the VLA-D is obvious but not as prominent as in the case of the snapshot mosaic.

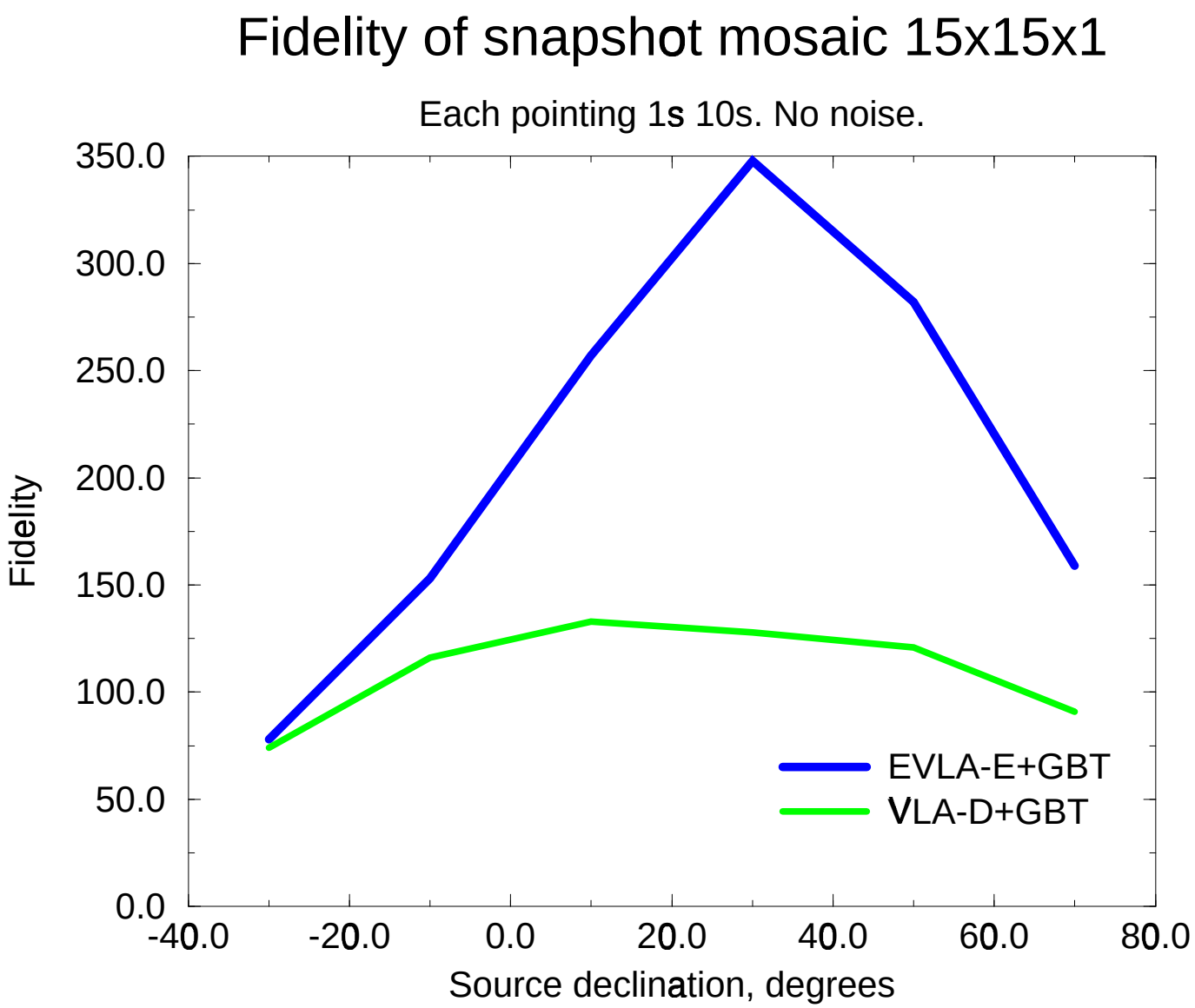

Figure 10: The fidelity versus the source declination for EVLA-E and VLA-D configurations for 15x15 snapshot mosaic. The advantage of the design compact configuration EVLA-E over the VLA-D is obvious but not so prominent as at the case of the 7x7 snapshot mosaic.

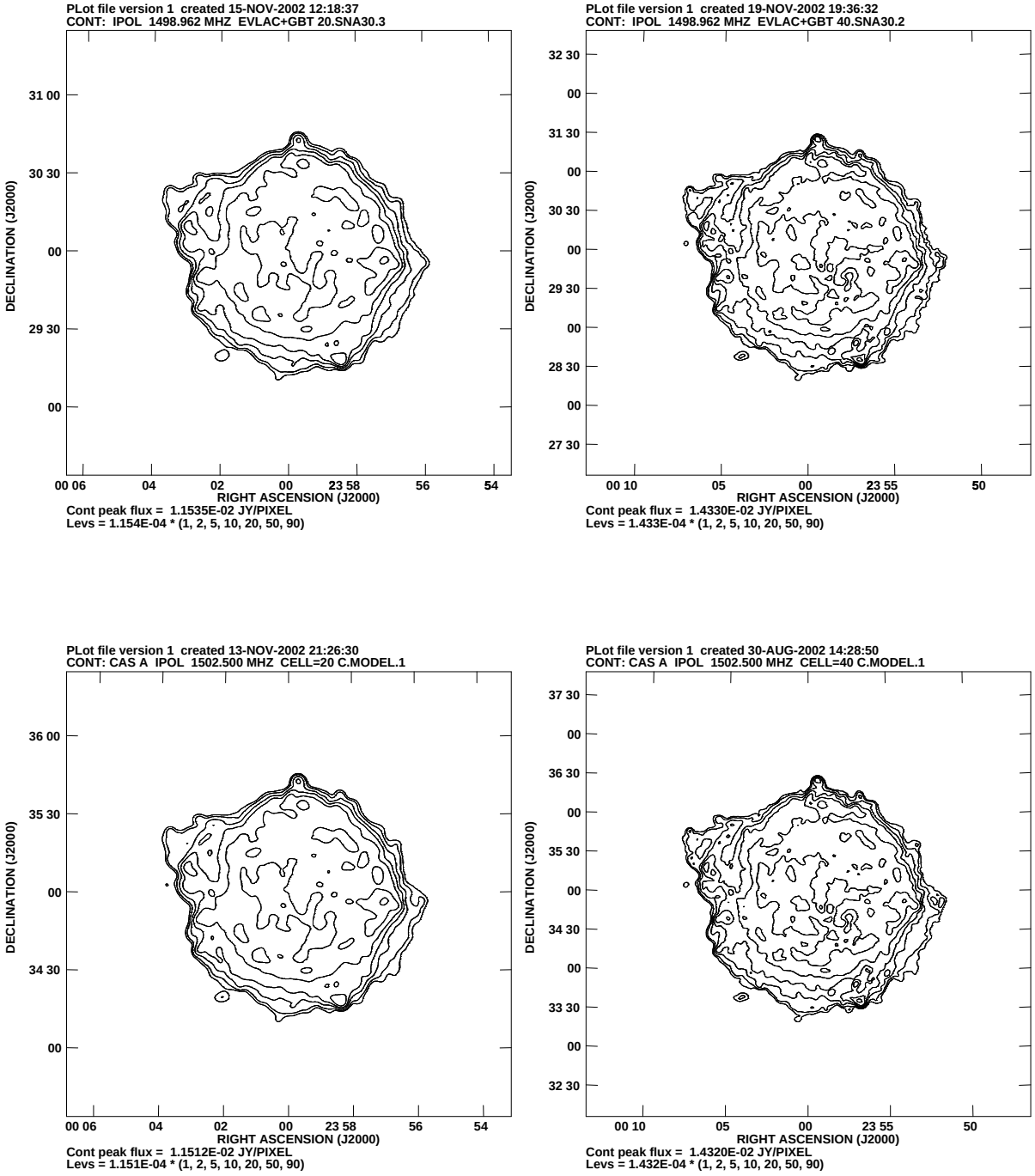

Figure 11: Illustration of the restored image quality for designed compact configuration EVLA-E. GBT observations are used to restore the hole at low UV. The left column shows 7x7 mosaic simulation corresponding to the model cellsize 20". The right column shows 15x15 mosaic simulation corresponding to the model cellsize 40". The upper row shows the restored images while the lower row shows the relevant models. **The restored images and the relevant models are practicaly identical at this scale.**

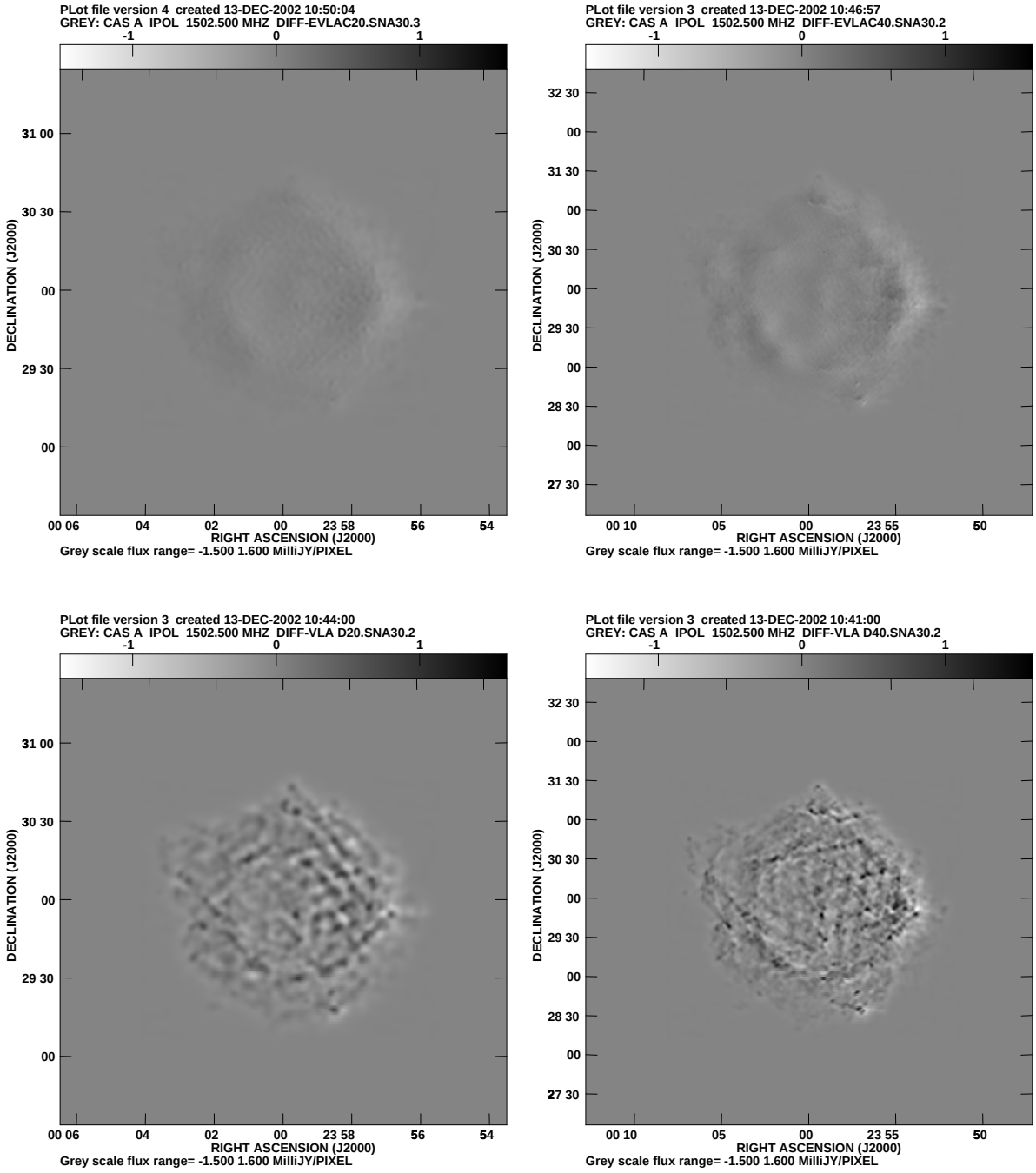

Figure 12: Images of differences of the restored images and the models for the two columns of the figure 11. As in figure 11 the left column shows 7x7 mosaic simulation corresponding to the model cellsize 20" and the right column shows 15x15 mosaic simulation corresponding to the model cellsize 40". The upper row shows the differences for the designed compact array EVLA-E. The lower row demonstrates the differences for the VLA-D array. Entire grey scale range of the low/right panel (-1.5,1.6 millijy/pixel) is chosen for all other panels to simplify the panel comparison. The model has maximum brightness ~ 14 millijy/pixel. **The advantage of the designed compact array EVLA-E over VLA-D array is obvious.**